

**A Growth Type Pathway for Improving the Folding of BPTI**

Journal:	<i>Organic & Biomolecular Chemistry</i>
Manuscript ID	OB-ART-05-2024-000802.R1
Article Type:	Paper
Date Submitted by the Author:	29-Jul-2024
Complete List of Authors:	Wang, Yingsong; Florida International University - Modesto A Maidique Campus, Chemistry and Biochemistry Mandumula, Shweta; Florida International University - Modesto A Maidique Campus, Chemistry and Biochemistry Lees, Watson; Florida International University - Modesto A Maidique Campus, Chemistry and Biochemistry

ARTICLE

A Growth Type Pathway for Improving the Folding of BPTI

Yingsong Wang, Shweta Mandumula, Watson J. Lees*

Received 00th January 20xx,
Accepted 00th January 20xx

DOI: 10.1039/x0xx00000x

The *in vitro* oxidative folding of the protein bovine pancreatic trypsin inhibitor (BPTI) with oxidized dithiothreitol or glutathione has served as a paradigm for protein folding but could take weeks at physiological pH because of the need to escape from kinetic traps via a rearrangement type pathway. The two major kinetic traps are called N* and N' and contain two of the three native disulfide bonds, which occur between residues 5 and 55, 30 and 51, and 14 and 38. N* is missing the disulfide bond between residues 5 and 55 while N' is missing the disulfide bond between residues 30 and 51. By determining rate constant for the reactions of the kinetic traps N* and N' and their mixed disulfides with glutathione and glutathione disulfide, many for the first time, we demonstrate that growth type pathways are feasible and could even be more efficient than rearrangement type pathways. Thus, formally unproductive pathways became productive. Interestingly, under physiological redox conditions both rearrangement and growth type pathways are important highlighting the redundancy of oxidative protein folding. With the new set of rate constants, modeling indicated that *in vitro* oxidative protein folding of BPTI via a growth type pathway using an oxidation, reduction and oxidation cycle would significantly improve protein folding efficiency, albeit under non-physiological redox conditions. With these changing conditions 91 ± 2% of native BPTI was achieved in 12 h compared to 83% native protein in 24 h using our previous best conditions of 5 mM GSSG and 5 mM GSH. Therefore, changing redox conditions via an oxidation, reduction and oxidation cycle may become an additional methodology for enhancing *in vitro* protein folding in aqueous solution.

Introduction

Oxidative protein folding is critical as almost all recombinant therapeutics contain disulfide bonds. One third of these proteins are produced in *E. coli*, many of which are folded *in vitro* (1). However, protein folding can be affected by the need to escape from kinetic traps (2-4). Three general pathways can be used to escape from kinetic traps formed during the oxidative folding of disulfide-containing proteins: rearrangement or reduction of disulfide bonds, or oxidation of protein thiols (Fig. 1, A to C) (5-8). If rearrangement of disulfide bonds is the escape mechanism and escape is the slowest step in the folding pathway then folding occurs via a rearrangement pathway while if thiol oxidation is the escape mechanism, then folding occurs via a growth type pathway as this leads to the formation of a new disulfide bond. The most efficient pathway will depend on several factors including subsequent folding steps, and the structure and stability of the kinetic traps.

The oxidative folding of bovine pancreatic trypsin inhibitor (BPTI) was proposed to follow almost exclusively a rearrangement type pathway (9-13). During oxidative folding, the six cysteine residues of reduced BPTI are oxidized to form three native disulfide bonds between residues 5 and 55, 30 and 51, and 14 and 38. As BPTI folds, only intermediates that contain native disulfide bonds accumulate and these are described by the disulfide bonds that they contain (Fig. 1D). A couple of the two-

disulfide intermediates act as kinetic traps, N* and N'. Intermediate N' contains disulfide bonds between 30 and 51, and 14 and 38, and is referred to as [30-51; 14-38], while N* contains disulfide bonds between 5 and 55, and 14 and 38, and is referred to as [5-55; 14-38]. Both N' and N* have two free thiols, structures like native protein, and slowly rearrange intramolecularly to N^{SH} [5-55; 30-51]. Under most conditions, the two remaining cysteines in N^{SH} are then rapidly oxidized to form the final disulfide bond and native protein, N. Since the slowest step in folding is a rearrangement step, this is referred to as a rearrangement type pathway. Direct oxidation of the two remaining cysteine thiols in N*, Cys30 and Cys51, to form N via a growth type pathway was initially reported not to occur due to the inaccessibility of the thiols (9,14) Direct oxidation of N' to N was reported to occur via the singly mixed disulfide of N' and GSH, N'(SG), however because of the rapid formation of the doubly mixed disulfide of N' with GSH, N'(SG)₂, from the reaction of GSSG with N'(SG) it was deemed inefficient (11). The N'(SG)₂ acts as a kinetic trap because it has no free thiols.

Department of Chemistry and Biochemistry, Florida International University,
Miami, FL 33199, USA. Email: leeswj@fiu.edu

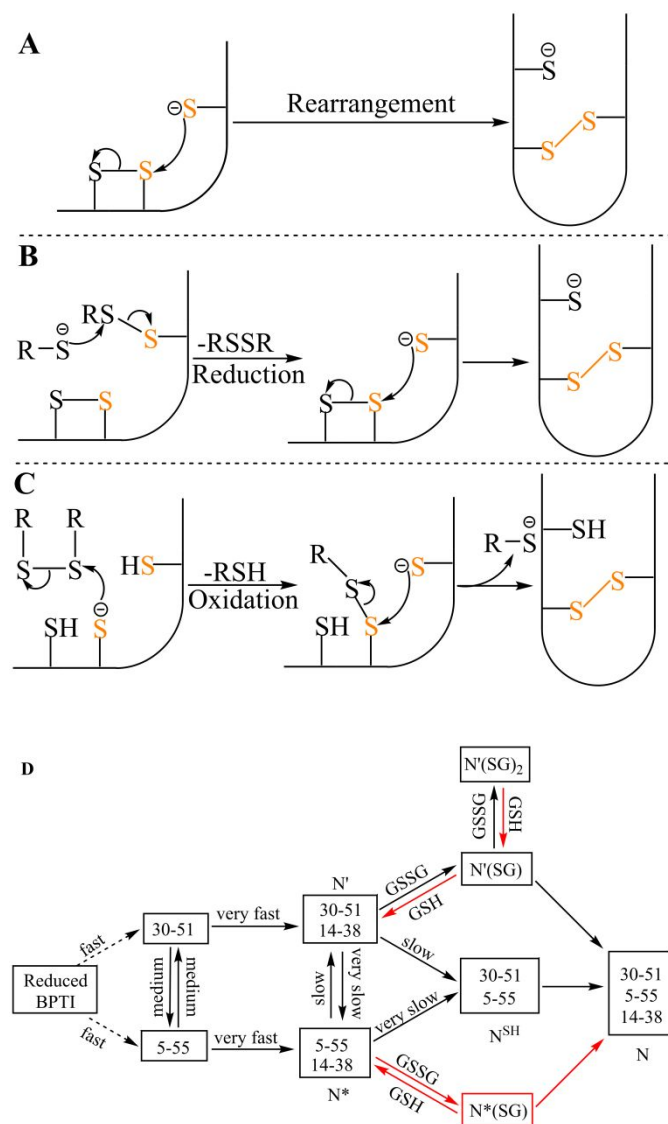


Fig. 1. Protein folding pathways. (A, B and C) Escaping from a kinetic trap via rearrangement, reduction, and oxidation. Sulfur in yellow indicates the correct atoms that will form the native disulfide bond. (D) Folding pathway of BPTI via both rearrangement and growth type pathways. The disulfide bonds of the protein intermediates are indicated inside the boxes. The relative rates at pH 7.3 are indicated; Reduced BPTI is oxidized initially to a mixture of one-disulfide intermediates which rapidly rearrange to [5-55] and [30-51]. Arrows in red indicate reaction pathways investigated herein.

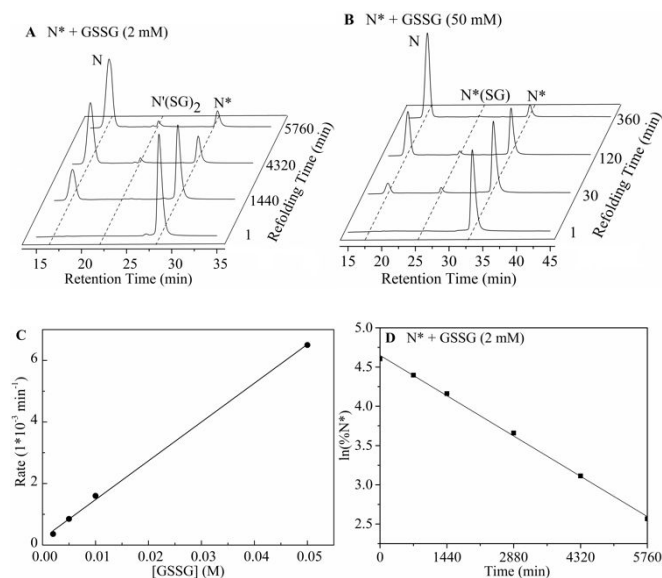
Recently, we followed the oxidative folding of reduced BPTI using a range of GSSG and GSH concentrations and proposed that the folding pathway involved the direct oxidation of the kinetic traps N^* and N' to N via growth type pathways (15). The importance of the N^* to N pathway was further supported by the folding of a modified form of BPTI (16). Traditionally, BPTI was folded using about 0.15 mM GSSG and no GSH or 0.5 mM GSSG and 2 mM GSH (10,17,18). However, our best conditions for folding BPTI were 5 mM GSSG and 5 mM GSH (15). Most interestingly when the folding of reduced BPTI with GSSG/GSH was modeled using a set of 17 rate constants the direct oxidation of N^* and N' to N , growth type pathways, were predicted to be significant. However, several of the rate constants were underdetermined. Herein, we isolate the kinetic traps, N^* and N'

and examine their reactivity, and elucidate more efficient folding conditions using GSH and GSSG.

Results

Oxidation and Reduction of N^*

The reaction of purified N^* (30 μ M) with GSSG was examined in buffer (0.1 M bis-tris propane at pH 7.3 with 0.2 M KCl and 1 mM EDTA) at 25 $^{\circ}$ C under argon (19). In the presence of 2, 5, 10 and 50 mM GSSG, N^* folded to N predominantly via a growth type pathway as the first order rate for the disappearance of N^* varied linearly with GSSG concentration, (Fig. 2). The GSSG concentrations were selected so that the reaction occurred in a reasonable amount of time and side reactions were minimized. In addition, the GSSG concentration would be much greater than any in situ generated GSH from reaction of GSSG with the protein (maximum 0.06 mM). Rates = 0.36×10^{-3} , 0.85×10^{-3} , 1.6×10^{-3} , and $6.0 \times 10^{-3} \text{ min}^{-1}$ respectively with second order rate constants of $k = 0.18$, 0.17, 0.16, and $0.12 \text{ M}^{-1}\text{min}^{-1}$, respectively, were determined. After make a small correction to the folding rate constants for the background rate due to the rearrangement of N^* to N' ($0.016 \times 10^{-3} \text{ min}^{-1}$ for 2 mM GSSG and $0.018 \times 10^{-3} \text{ min}^{-1}$ for 5 mM GSSG, $0.019 \times 10^{-3} \text{ min}^{-1}$ for 10 mM, see below) the rate constants became 0.17, 0.17, 0.16 and $0.12 \text{ M}^{-1}\text{min}^{-1}$, respectively. If the direct intramolecular rearrangement of N^* to N' or N^{SH} was rate determining, as reported previously, then the folding rate should be almost independent of the GSSG concentration as direct intramolecular rearrangement does not involve GSSG. The addition of GSH did not increase the reaction rates for 10 or 50 mM GSSG, see below.



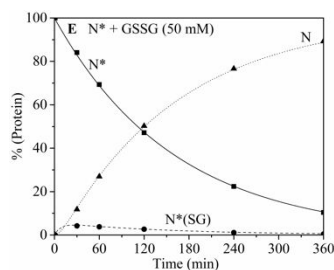


Fig. 2. HPLC chromatograms obtained from folding of N^* with (A) 2 mM GSSG and (B) 50 mM GSSG after various refolding times. (C) Folding rates of N^* with different concentrations of GSSG. (D) Determination of folding rate at 2 mM GSSG by following loss of N^* , $0.36 \times 10^{-3} \text{ min}^{-1}$. (E) Comparison of experimental results with modeled results for the folding of N^* at 50 mM GSSG.

Minor side products were observed when N^* was reacted with 2 and 50 mM GSSG. With 2 mM GSSG a small amount of the doubly mixed disulfide $N'(SG)_2$ was observed due to the rearrangement of N^* to N' , $k = 2 \times 10^{-5} \text{ min}^{-1}$, followed by the relatively rapid reaction of N' with two equivalents of GSSG to form $N'(SG)_2$ (Fig. 2A). The rate constant was adjusted for the fact that the folding of N' in the presence of 2 mM GSSG produced 46% $N'(SG)_2$ as N' can also rearrange back to N^* or to N^{SH} . With 50 mM GSSG a species kinetically consistent with $N^*(SG)$ and of the appropriate molecular weight was observed (Fig. 2B). Analogues of $N^*(SG)$ have been reported previously (16,20), such as the selenium analogue and a modified version of BPTI in which the 14-38 disulfide bond was in effect fixed in place. After modelling, the rate constant for the $N^*(SG)$ to N reaction was determined to be 0.12 min^{-1} . To examine the effect of GSH concentration on the conversion of N^* to N , five conditions were compared 10 mM GSSG with 0, 10, and 20 mM GSH, and 50 mM GSSG with 0 and 35 mM GSH. Although the addition of GSH decreased the N^* to N conversion rate, the effect was small (50% with 35 mM GSH) and indicated a back reaction of $N^*(SG)$ to N^* with a rate constant of approximately $3 \text{ M}^{-1} \text{ min}^{-1}$. Due to the reduction of N^* with GSH, a side reaction, a more accurate rate constant for the $N^*(SG)$ to N^* reaction was obtained when the GSSG concentration is higher than GSH concentration. The reduction rate of N^* with GSH was also examined (Fig. 3) at 50 mM GSH.

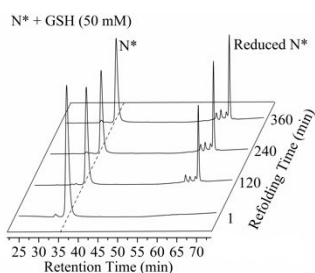


Fig. 3. HPLC chromatograms obtained from reduction of N^* with 50 mM GSH at various reaction times.

Oxidation and reduction of N' , $N'(SG)$, reduction of $N'(SG)_2$, and rearrangement of $N'(SG)$,

Folding via a growth type pathway was also shown to be important for the second kinetic trap N' . Initially, the rate

constants for the relevant reactions were determined. In the presence of 20 mM GSSG, N' was converted almost exclusively to $N'(SG)_2$ due to the relatively rapid reaction of $N'(SG)$ with GSSG, although the rate determining step was the conversion of N' to $N'(SG)$ (Fig. 4A). Due to the enhanced reactivity of $N'(SG)$ relative to N' , $N'(SG)$ was reacted with 2 mM GSSG to form $N'(SG)_2$ (Fig. 4B). The reduction of $N'(SG)_2$ to $N'(SG)$ proceeded smoothly at 0.5 mM GSH (Fig. 4C). The reduction of $N'(SG)$ and N' with GSH produced a mixture of intermediates (Fig. 4D and 4E, respectively). The rearrangement of $N'(SG)$ to N was also followed (Fig. 5) Upon modelling, the reduction of $N'(SG)$ with GSH, it became clear that the GSH was reacting with $N'(SG)$ in at least two places, the mixed disulfide and one or both native disulfide bonds. Thus, an additional reaction was incorporated into the model (Fig. 6). The reactivities of the native disulfide bonds in N' and $N'(SG)$ towards GSH were similar. The rate constants were within 40% of those reported previously: N' to $N'(SG)$: 2.5 versus $3 \text{ M}^{-1} \text{ min}^{-1}$; $N'(SG)$ to $N'(SG)_2$: 80 versus $90 \text{ M}^{-1} \text{ min}^{-1}$; $N'(SG)$ to N : 2.2 versus $2.8 \times 10^{-3} \text{ min}^{-1}$; N' to N^* : 1.7 versus $1.2 \times 10^{-3} \text{ min}^{-1}$; N' to N^{SH} : 1.9 versus $1.5 \times 10^{-3} \text{ min}^{-1}$ (11) and the equilibrium constant between N' and N^* of 85 was somewhat higher than the value of 33 determined at pH 8.7 between N^* and a mixture containing mainly N' (9)

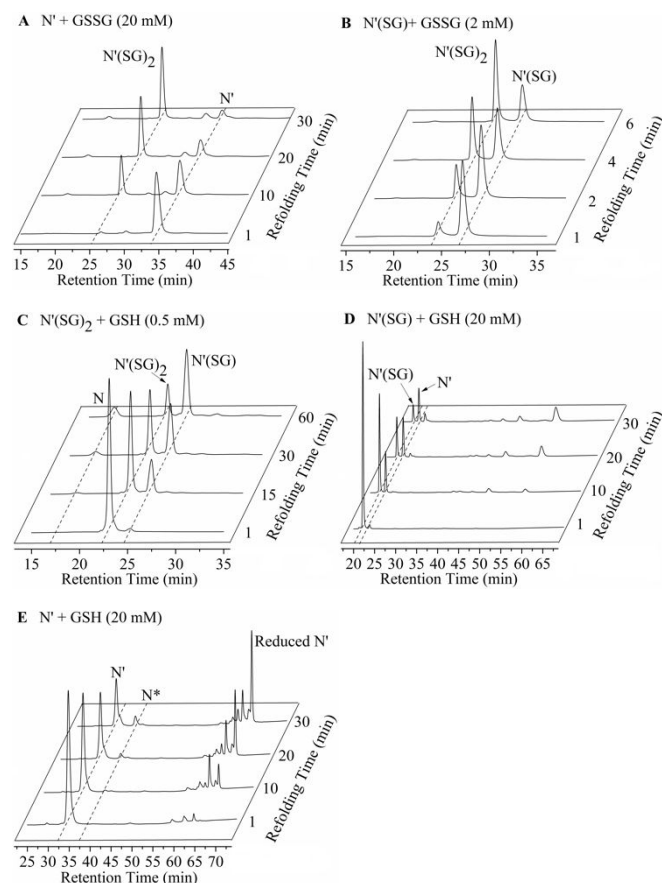


Fig. 4. HPLC chromatograms obtained from reactions of intermediates with GSSG or GSH after various reaction times.

N'(SG) with GSSG to form N'(SG)₂, however, under conditions where the GSSG and GSH concentrations are similar, the N'(SG)₂ will be rapidly converted back to N'(SG) with an equilibrium constant of 1.5, as determined herein (11). Both our best conditions for folding reduced BPTI (5 mM GSSG and 5 mM GSH) and those found in the endoplasmic reticulum, ER, (5 mM protein mixed disulfides with GSH (PSSG), 3 mM GSH, and 1 mM GSSG) have similar concentrations of GSSG or equivalent (0.5[PSSG]), and GSH (15, 21). The equilibrium constant between N'(SG) + GSSG and N'(SG)₂ + GSH is 1.5 and the rate constant for the conversion of N'(SG) to N is 1.15 times that of the N' to N rate constant. Therefore, when the concentrations of GSH and GSSG are identical, the rate at which an equilibrium mixture of N'(SG) and N'(SG)₂ (40:60 ratio) is converted to native protein via a growth type pathway will be 46% (40% × 1.15) that of N' to N via a rearrangement type pathway. For the growth type pathway, the rate determining step will be N'(SG) to N, while for the rearrangement type pathway the rate determining step will be N' to N^{SH}. Thus, folding N' to native protein via both types of pathways is important.

Effective concentration can be used to compare the intramolecular reaction rate of a protein intermediate versus the intermolecular reaction rate with a small molecule disulfide such as GSSG. For N*, the intramolecular rearrangement rate constant of N* to N' was $2 \times 10^{-5} \text{ min}^{-1}$, k_{intra} , while the intermolecular reaction rate constant with GSSG was $0.15 \text{ M}^{-1}\text{min}^{-1}$, k_{inter} , corresponding to an effective concentration ($k_{\text{intra}}/k_{\text{inter}}$) of 0.13 mM GSSG. Therefore, the major reaction for N* changes at about 0.13 mM GSSG from being a rearrangement reaction to being a growth type reaction. Thus, under the traditional conditions used to study the folding of BPTI, 0.125 mM GSSG the major folding pathways for N* likely involved intramolecular rearrangement of disulfide bonds, as reported, while under our more efficient folding conditions, 5 mM GSSG and 5 mM GSH, the major folding pathway for N* is a growth type pathway, direct reaction of N* with GSSG. Therefore, at low GSSG concentrations where the rearrangement pathway dominates the rate determining step will be the rearrangement of N* to N' but at higher GSSG concentrations where the growth type pathway dominates the rate determining step will be the reaction of N* with GSSG. For N', the ratio of the rate constants for rearrangement to N^{SH} versus reaction with GSSG, effective concentration, was reported previously to be 0.5 mM (11) and determined herein to be 0.8 mM.

The most efficient *in vitro* folding pathway of BPTI may be accomplished via what has traditionally been called the non-productive route. Rearrangement of N' to N or conversion of N'(SG) to N is limited by a first order rate constant of approximately 0.002 min^{-1} . Rearrangement of N' to N*, produces a more thermodynamically stable kinetic trap, however, the rate determining step in the conversion of N* to N is determined by a second order rate constant and at GSSG concentrations above 15 mM the N* to N reaction becomes faster than the rearrangement of N' to N^{SH}. Ultimately, due to the rapid conversion of N*(SG) to N, the most efficient way to fold N' may be via N* at high GSSG concentrations, which was historically

called the non-productive route, and not via rearrangement of N', which was traditionally called the productive route.

Having determined many of the rate constants for the later stages of BPTI folding, we predicted that changing folding conditions with folding time would improve the folding efficiency of BPTI, and we were able to produce $91 \pm 2\%$ N in 12 h, within error of the predicted 89% (Fig. 8A). Previously, we were able to produce 83% native protein in 1 day with 5 mM GSSG and 5 mM GSH at pH 7.3 (15). Using the selenium analogue of glutathione, glutathione diselenide (GSeSeG), Hilvert et al. was able to produce approximately 95% native protein in 1 day at pH 7.3 (20), and if a seleno analogue of the protein was used as well then 85% folded protein could be produced in 6 h (22). The GSeSeG also increases the N* to N rate, maybe via a growth type pathway as N*(SeG) was observed (20). Using a BPTI analogue in which the 14-38 disulfide bond was fixed, species corresponding to N*(SG) and N*(SG)₂ were reported albeit at higher pH (8.7) and much lower GSSG concentrations (0.1 mM GSSG) (16). Because the 14-38 disulfide bond was fixed the species corresponding to N' could only go to a species corresponding to N* and not the one corresponding to N^{SH}. Higher pH values can make buried thiols more accessible. At 50 mM GSSG, we did not observe a significant species that was kinetically consistent with N*(SG)₂, as this would be expected to be a very stable kinetic trap like N'(SG)₂, (Figs. 2 and 4). In organic solvents BPTI can fold to 62% native protein in under a second, although the pathway is unclear (23,24). The addition of other small molecule reducing agents besides GSH/GSSG can also be beneficial (25-27).

Experimental

Preparation of reduced BPTI and kinetic traps

Native BPTI was purchased as aprotinin in ultra-pure grade from Roche Applied Science. Reduced BPTI was prepared by denaturing native BPTI according to previous methods (19,28). Kinetic traps N*, N', and N'(SG)₂ were prepared by reaction of reduced BPTI (30 μM) with different concentrations of GSSG/GSH under argon at 25 °C, 0.125 mM GSSG and 20 mM GSH for 48 h to produce N*, 0.5 mM GSSG and 5 mM GSH for 15 min to produce N', 20 mM GSSG for 6 h to produce N'(SG)₂, respectively, in the presence of deoxygenated bis-tris propane buffer (0.1 M bis-tris propane, 0.2 M KCl and 1 mM EDTA) at pH 7.3. The buffer solution was deoxygenated by flowing argon through it for 30 min prior to the addition of reduced BPTI. Intermediate N'(SG) was obtained by reduction of N'(SG)₂ (30 μM) with 10 mM GSH in deoxygenated buffer for 6 min under argon at 25 °C. All reaction mixtures were quenched by addition of 1/20th by volume of formic acid to the folding mixture, desalted on a Sephadex G-25 column using 0.01 N HCl as the mobile phase, lyophilized, dissolved in 0.01 N HCl, and injected onto a HPLC Vydac C18 semi-preparative column (218TP510, 250 × 10 mm) maintained at 50 °C. The HPLC solvent was a mixture of 0.1% trifluoroacetic acid in water (solvent A) and 90% vol/vol acetonitrile in water with 0.1% trifluoroacetic acid (solvent B). The absorbance was monitored at 280 nm. Purification of all intermediates was performed using the

following linear gradient with a flow rate of 3 mL/min: 0 min, 90% solvent A; 15 min, 75% solvent A; 35 min, 73% solvent A; 50 min, 72% solvent A; 100 min, 65% solvent A. The purity of each protein fraction was determined on a Vydac C18 analytical column (218TP54, 250 × 4.6 mm) maintained at 50 °C and the absorbance was monitored at 229 nm. A linear gradient with a flow rate of 1 mL/min was used: 0 min, 90% solvent A; 15 min, 75% solvent A; 35 min, 73% solvent A, 50 min, 72% solvent A; 70 min, 69% solvent A. Pure protein fractions were lyophilized, dissolved in 0.01 N HCl, combined and stored at -20 °C.

Oxidative folding of intermediates with GSSG

Reactions of N*, N' and N'(SG) (30 μM) with GSSG were conducted in bis-tris propane buffer (0.1 M bis-tris propane, 0.2 M KCl, and 1 mM EDTA) at pH 7.3 under argon at 25 °C. At specific times, 300 μL aliquots were removed and quenched by the addition of 15 μL of formic acid. All aliquots were kept in a refrigerator at 4 °C prior to HPLC analysis. Each aliquot was analysed by HPLC on a Vydac C18 analytical column (218TP54, 250 × 4.6 mm) as described above.

Reduction of intermediates with GSH

Reduction of N'(SG)₂, N'(SG), N' and N* (30 μM) with GSH was conducted as for GSSG. However, the HPLC gradient used was different: 0 min, 90% solvent A; 15 min, 75% solvent A; 35 min, 73% solvent A; 50 min, 72% solvent A; 100 min, 50% solvent A.

Rearrangement of intermediates

Rearrangement reactions of two intermediates, N' and N'(SG), were performed in bis-tris propane buffer alone (0.1 M bis-tris propane, 0.2 M KCl and 1 mM EDTA) at pH 7.3 under argon at 25 °C. The HPLC gradient used was the same as for GSSG.

Determination of rate constants for the reactions of kinetic traps

The peaks for N, N*, N', N'(SG), and N'(SG)₂ were assigned based upon precedent (10,11,17,29). The concentration of each peak was derived from its relative peak area. The kinetic scheme used for modelling of BPTI folding is shown in Fig. 7. The reverse kinetic problem was solved by fitting rate constants of all the reaction steps involved to reproduce experimental concentration profiles using Euler's method (15) ($\Delta t = 0.1$ s for reactions less than 6 h and 1 s for reactions more than 6 h). For a certain folding reaction, only the relevant rate constants involved in the reaction steps were used. The following reactions were modelled and used to determine the rate constants: rearrangement of N' (k_4 and k_5), reaction of N'(SG)₂ with GSH (k_{-8} , a 30% increase over pseudo first order kinetics due to low GSH concentration (0.5 mM) and in situ generation of a small amount of GSSG, up to approximately the protein concentration of 0.03 mM, that causes the back reaction), reaction of N* with high GSSG concentration with and without GSH (k_9 and k_{11}), and reaction of N'(SG) with GSH (k_7 and k_{13}). Rate constants k_2 (disappearance of N'), k_3 (disappearance of N*), k_7 (disappearance of N'), k_8 (disappearance of N'(SG)), k_9 (disappearance of N*), and k_{10} (formation of N) were determined using pseudo first order kinetics.

Folding under changing conditions

The folding reaction was followed by characterizing the aliquot quenched with formic acid at each specific time. Each aliquot was analyzed by HPLC on a Vydac C18 analytical column. The absorbance was monitored at 229 nm and the column temperature was maintained at 50 °C. A flow rate of 1 mL/min linear gradient was used: 0 min, 90% solvent A; 15 min, 75% solvent A; 35 min, 73% solvent A; 50 min, 72% solvent A; 110 min, 70% solvent A. For changing conditions at 15 minutes only, the initial reaction contained 5 mM GSH and 2 mM GSSG. At 15 min, a 0.3 mL aliquot was removed for analysis and replaced with 200 mM stock solutions of GSH (0.41 mL) and GSSG (0.65 mL) in buffer. For changing conditions at 15 min and 1 h the initial reaction contained 5 mM GSH and 2 mM GSSG. At 15 min, a 0.30 mL aliquot was removed for analysis and replaced with 200 mM GSH (0.30 mL) in buffer. At 1 h, a 0.30 mL aliquot was removed for analysis and replaced with 200 mM GSSG (0.54 mL) in buffer.

Conclusions

We have updated the *in vitro* oxidative folding pathway of BPTI and demonstrated that BPTI can fold efficiently not only via rearrangement type pathways but also via growth type pathways with GSSG and GSH. The ability to fold BPTI via both a growth and rearrangement type pathway to N indicates a very robust system. Folding of reduced BPTI via N*, historically the non-productive route, was shown to be more efficient than folding via N' at high GSSG concentrations. The production and folding of N* were enhanced by folding under changing concentrations of GSSG and GSH with time. Folding under changing condition may prove to be a general strategy for improving protein folding efficiency.

Author Contributions

Y. Wang and S. Mandumula performed the folding experiments and data analysis. Y. Wang wrote and edited the manuscript. W. J. Lees supervised the project, edited the manuscript and obtained the funding.

Conflicts of interest

There are no conflicts to declare.

Data Availability

The data supporting this article have been included as part of the Supporting Information.

Acknowledgements

Financial support from the NSF (Grant CHE-0342167 to WJL) is gratefully acknowledged. We thank Dr. Bruce McCord and Hanzhuo Fu for their helpful advice.

Notes and references

1. C. Huang, Jr., H. Lin and X. Yang, *J. Ind. Microbiol. Biotechnol.* 2012, **39**, 383-399.
2. M. Narayan *Molecules*, 2020, **25**, 5337-55.
3. K. Arai and M. Iwaoka, *Molecules*, 2021, **26**, 195-213.
4. M. Narayan, *J. Phys. Chem. B* 2022, **126**, 10273-10284.
5. Y. Konishi, T. Ooi and H. A. Scheraga, *Proc. Natl. Acad. Sci. U. S. A.* 1982, **79**, 5734-5738.
6. Y. Konishi, T. Ooi and H. A. Scheraga, *Biochemistry* 1982, **21**, 4734-4740.
7. Y. Konishi, T. Ooi and H. A. Scheraga, *Biochemistry* 1982, **21**, 4741-4748.
8. H. A. Scheraga, Y. Konishi and T. Ooi, *Adv. Biophys.* 1984, **18**, 21-41.
9. T. E. Creighton and D. P. Goldenberg, *J. Mol. Biol.* 1984, **179**, 497-526.
10. J. Weissman and P. Kim, *Science* 1991, **253**, 1386-1393.
11. J. S. Weissman and P. S. Kim, *Nat. Struct. Mol. Biol.* 1995, **2**, 1123-1130.
12. T. Creighton, *Science* 1992, **256**, 111-112.
13. J. S. Weissman and P. S. Kim, *Science* 1992, **256**, 112-114.
14. D. J. States, C. M. Dobson, M. Karplus and T. E. Creighton, *J. Mol. Biol.* 1984, **174**, 411-418.
15. F. M. Kibria and W. J. Lees, *J. Am. Chem. Soc.* 2008, **130**, 796-797.
16. R. Mousa, S. Lansky, G. Shoham and N. Metanis *Chem. Sci.*, 2018, **9**, 4814-4820.
17. A. Zapun and T. E. Creighton, *Biochemistry* 1994, **33**, 5202-5211.
18. J. S. Weissman and P. S. Kim, *Cell*, 1992, **71**, 841-851.
19. J.-X. Zhang and D. P. Goldenberg, *Protein Sci.*, 1997, **6**, 1549-1562.
20. N. Metanis, C. Foletti, J. Beld and D. Hilvert, *Isr. J. Chem.*, 2011, **51**, 953-959.
21. R. Bass, L. W. Ruddock, P. Klappa and R. B. Freedman, *J. Biol. Chem.* 2004, **279**, 5257-5262.
22. N. Metanis and D. Hilvert, *Angew. Chem. Int. Ed.* 2012, **51**, 5585-5588.
23. A. Kam, S. Loo, Y. Qiu, C.-F. Liu, and J. P. Tam, *Angew. Chem. Int. Ed.*, 2024, **63**, e202317789.
24. S. Laps and N. Metanis, *Nat. Chem.*, 2024, **117**.
25. H. Nishino, M. Kitamura, S. Okada, R. Miyake, M. Okumura and T. Muraoka, *RSC Adv.*, 2022, **12**, 26658-26664.
26. S. Okada, Y. Matsumoto, R. Takahashi, K. Arai, S. Kanemura, M. Okumura and T. Muraoka, *Chem. Sci.*, 2023, **14**, 7630-7636.
27. T. Muraoka, M. Okumura and T. Saio, *Chem. Sci.*, 2024, **15**, 2282-2299.
28. J.-X. Zhang and D. P. Goldenberg, *Protein Sci.*, 1997, **6**, 1563-1576.
29. J. S. Weissman and P. S. Kim, *Nature*, 1993, **365**, 185-188.

Data Availability for**A Growth Type Pathway for Improving the Folding of BPTI**

Yingsong Wang, Shweta Mandumula, Watson J. Lees

The data supporting this article have been included as part of the Supplementary Information.